Asian Journal of Chemistry; Vol. 34, No. 6 (2022), 1443-1450

ASIAN JOURNAL OF CHEMISTRY

https://doi.org/10.14233/ajchem.2022.23711

Design, Synthesis and Pharmacological Assay of Sulfadiazine based Azo-Metal Complexes

H.B. TEJA[1], H.S. BHOJYA NAIK[1,*], P.H. AMITH NAYAK[1], R. VISWANATH[1], K. VINU[2] and U. HANI[3]

[1]Department of P.G. Studies and Research in Industrial Chemistry, School of Chemical Science, Kuvempu University, Shankaragatta- 577451, India
[2]Department of Applied Botany, Kuvempu University, Jnana Sahyadri, Shankaraghatta-577451, India
[3]Department of Biotechnology, Kuvempu University, Jnana Sahyadri, Shankaraghatta-577451, India

*Corresponding author: E-mail: hsb_naik@rediffmail.com

Received: 4 January 2022; *Accepted*: 25 February 2022; *Published online*: 18 May 2022; AJC-20804

This study reported the biologically active Cu(II), Co(II) and Ni(II) complexes of the novel azo dye ligand pyrimidin-2-yl-4-[(*E*)-(2,4,6-trioxohexahydropyrimidin-5-yl)diazenyl]benzenesulfonamide. The structures of synthesized metal complexes were established on spectroscopic and physico-chemical techniques. From the spectral studies, it confirms that the azo ligand coordinates to the metal center through a bidendate manner *via* barbutaric acid -OH, azo-N as a donor site. The thermal studies reveals that all the complexes exhibits good thermally stability and also the presence of water molecule for Co(II) and Ni(II) complexes. The prepared metal chelates have been examined for their antibacterial activity against *Staphylococcus aureus, Xanthomonas campestris, Klebsiella pneumonia and E. coli* by using agar well diffusion method. The data revealed the ability of the complexes to inhibit the growth of some microorganisms, among all the compounds Co(II) complex showed the highest activity. The antifungal activity of the compounds were tested against two strains, whereas Ni(II) complex showed the highest activity against fungal strains. Lastly, the probable binding sites of metal complexes with receptor RpsA were studied by molecular docking studies.

Keywords: Azo-metal chelates, Thermal studies, Antibacterial activity, Molecular docking.

INTRODUCTION

Sulfa drugs are the most extensively used antimicrobial agents in the world, because of their low cost, low toxicity; sulfonamides have also played an vital role as antibacterial, antifungal, anticancer antimalarial and antituberculosis agents [1]. The pharmacological activity of sulfadiazine is because of its structure resemblance between the sulfanilamide group and the *p*-aminobenzoic acid, which prevents the synthesis of folic acid path and blocks the cell division, causing cell death [2]. Azo dyes are owning at least one conjugated chromophoric azo linkage (-N=N-) next to one or more heterocyclic or aromatic moieties in their structures. Sulfonamide's azo dyes have been reported to possess antimicrobial activity [3], antiinflammatory activity [4] and antitumor activity. The sulfonamides azo derivatives shown anti-infectious properties. Furthermore, barbituric acid is one of the most fascinating derivatives of pyrimidines. Barbituric acid is mainly derived from barbiturate drugs, although barbituric acid himself is not bioactive, and the bioactivity of barbiturates mainly depends on the side groups attached to the C-5 atom of the pyrimidine ring [5]. Both sulfadiazine and barbutaric acid have donor atoms (N and O) at different positions, and this will enhance them to act as multidentate ligands. Hence, they can coordinate with different metal ions [6,7]. It was seen that after the coordination with the metal ion the pharmacological activity of the azo dye have been improved. The activity of the sulfonamide metal complexes was depended on the gentle release of metal ions and also more prominently, depends on the nature of the molecules to which the metal ion is bound [8]. Therefore, coordination of sulfa drugs to these important metals leads to important biological purposes.

In this direction, the synthesis of some novel azo dyes derived from sulfadiazine and their Cu(II), Co(II) and Ni(II) metal complexes were carried out. The structures of the newly synthesized metal chelates were confirmed by physico-chemical and spectral techniques. The antimicrobial and molecular docking studies of the azo metal complexes were studied in order to evaluate their potency to inhibit the respective pathogens.

EXPERIMENTAL

Metal(II) salts, barbutaric acid, sulfadiazine were procured from Sigma-Aldrich, USA. Other chemicals and solvents were of highest purity and used without further purification. The NMR spectra were recorded on a Bruker 400 MHz High Resolution Multinuclear FT-NMR Spectrometer at 25 ºC using DMSO as solvent and TMS as an internal reference. The FT-IR spectra were recorded with a thermo nicolet avatar IR spectrophotometer using KBr pellets. The UV-visible spectra were obtained on shimadzu model 1650 UV-Visible double beam spectrometer in DMF solution (10^{-3} M). Elemental analyses (C,H,N) were performed by using Perkin-Elmer 2400. The mass spectra of the compounds were recorded on LC-MS: water AQUITY-2777C mass spectrometer. The thermal analyzer was recorded as TG-DSC curves. The surface morphology of the synthesized compounds were determined by Zeiss scanning electron microscope. The powdered XRD was recorded on Bruker AXS D8 prior instrument.

Synthesis of azo dye ligand (L): The azo dyes were synthesized according to the reported procedure [9]. A cold solution of sulfadiazine (0.1 mol) in conc. HCl (5 mL) was added dropwise to a cold sodium nitrate (0.1 mol) in 10 mL of ice cold water with constant stirring, the resulting mixture was stirred for 1 h. The temperature of the mixture was maintained at 0 to 5 ºC, the coupling component barbutaric acid (0.1mol) was dissolved 10 mL of KOH solution, which was cooled in ice bath. The mixture was gradually added to the diazonium salt solution and the resulting mixture was stirred again for 2 h at same temperature. The pH of the reaction mixture was maintained at 5-6 by adding saturated sodium bicarbonate solution. The obtained coloured dye was filtered, washed with cold water several times, dried and recrystallized using absolute ethanol (**Scheme-I**).

Synthesis of azo metal complexes (1a-c): The synthesized azo dye (0.2 mol) and metal(II) hydrates (0.1 mol) were dissolved in absolute ethanol and the resulting solution was refluxed for 4-5 h with constant stirring at 60 ºC. After that the reaction mixture was allowed to stand overnight. A coloured solution was filtered and washed with distilled water-ethanol mixture and dried over anhydrous $CaCl_2$ in a vacuum desiccator [10].

Antimicrobial studies: The synthesized metal complexes were screened for their antimicrobial activity against *Staphylococcus aureus*, *Escherichia coli*, *Santhomonas ampestris*, *Klebsiella pneumonia* and antifungal activity against *Candida albicans* and *Aspergillus flavus* by agar well diffusion method. Briefly, the microorganism inoculums were evenly spread using sterile cotton swab on a sterile petri dish containing malt agar (for fungi) and nutrient agar (for bacteria). Different concentration of metal chelates was added to each well (6 mm diameter holes cut in the agar gel, 20 mm apart from one another). The plates were incubated for 24-48 h at 37 ºC (for bacteria) and at 28 ºC (for fungi). After incubation, microorganism growth was observed. Inhibition of the bacterial and fungal growth were measured in mm. Tests were performed in triplicate. The minimal inhibitory concentration (MICs) was determined after incubation period [11].

Molecular docking: MGL tools 1.5.4 with AutoDock4 were used to perform blind docking calculations. The structures of synthesized molecules were drawn using ChemSketch software and convert it into PDB format from mol format by online OPENBABEL. The DNA sequence d(ACCGACGTCGGT)2 found from the Protein Data Bank (PDB id: 423D) at a resolution of 1.60 Å was used for the docking studies. First of all the water molecules were deleted, polar hydrogen and Kollman charges were added, non-polar hydrogens were merged into their analogous carbons using AutoDock tool, then rotatable bonds in ligands were assigned. All the intentions were carried out on an Intel Pentium 4, 2.4 GHz based machine running MS Windows XP SP2 as operating system. The output results from AutoDock were analysed by ligplot and paymol software. According to the autodock score, the lowest energy docked conformation was selected as the binding mode.

RESULTS AND DISCUSSION

NMR studies: ^{1}H NMR spectra of the free ligand was recorded using DMSO as a solvent. The azo ligand showed a singlet at δ 13.97 ppm, which is clearly attributed to NH of sulfadiazine. The singlet at δ 11.8 ppm was attributed to NH of azo group [12]. A signal corresponds to hydrogen devoted to nitrogen of the pyrimidinetrione ring was observed at δ 11.57

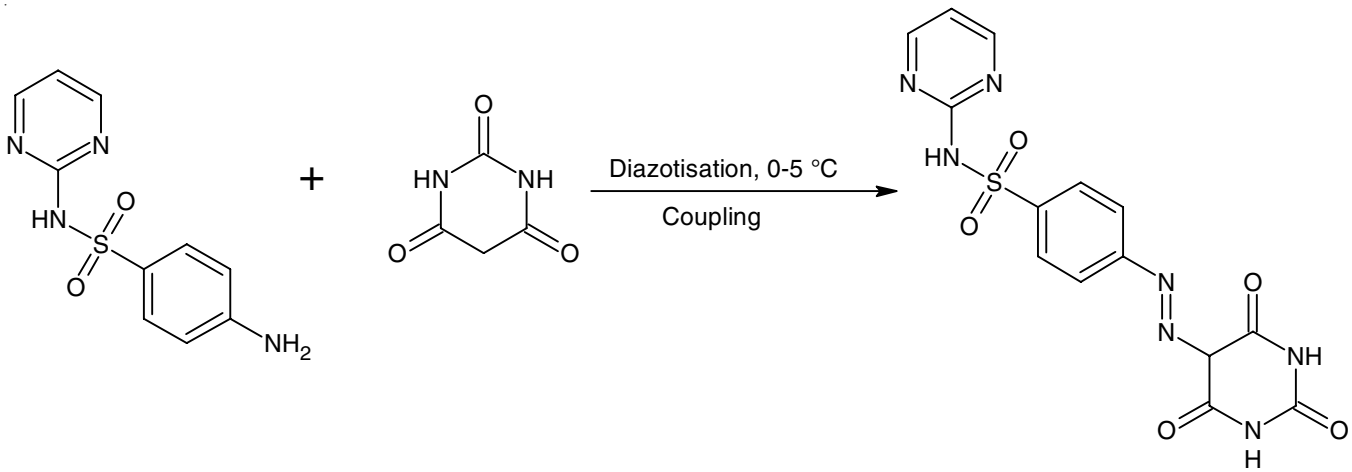

Scheme-I: Synthetic route for azo dye ligand (L)

and 11.35 ppm. The aromatic protons show signals at δ 7.68-8.48 ppm [13]. The ^{13}C NMR spectra of free ligands showed a signal at δ 162, 160 and 158 ppm corresponds to carbon of the pyrimidine ring [14]. The signals at δ 158.6, 157.2, 150.1 ppm corresponds to C=O of the pyrimidinetrione ring. The aromatic region corresponds to δ 112-136 ppm.

Mass studies: The mass spectrum of azo ligand and its metal(II) complexes showed a molecular ion peak analogous to their molecular mass. The mass spectrum of azo ligand exhibited a apparent molecular ion peak observed at *m/z* 389 [M+H], which is similar to its molecular mass of the ligand. In addition, the mass spectra of Cu(II), Co(II) and Ni(II) complexes will display a molecular ion peak at *m/z* 840,871,835 respectively, which are synchronized with the stoichiometric configuration of $[ML_2]$ type. Additionally, the observed molecular ion peaks in all the spectra are in good agreement with the recommended molecular formula indicated from elemental analyses.

FT-IR Studies: The IR spectrum of azo ligand showed the strong bands at 1725, 1682, 1596 cm^{-1}, which corresponds to the ν(C=O) vibrations of the barbutaric acid [15]. A strong absorption at 1431 cm^{-1}, which can be assigned to the N=N group and a medium intense band at 1245 and 1151 cm^{-1} corresponds to the ν_{asym} and ν_{sym} of the (O=S=O) moiety, the other bands observed at 3084 and 2822 cm^{-1} due to aromatic ν(C-H) and aliphatic ν(C-H), respectively. In the spectra of the synthesized metal chelates, the two carbonyl carbons appear in the region of 1724-1587 cm^{-1} and the third carbonyl carbon disappeared in all the metal complexes [16]. The appearance of new band at 1135-1107 cm^{-1} for the metal complexes attributed to C-O vibration, which indicates the coordination through carbonyl carbon of the barbuaric acid. The absorption band with in the range 1431 cm^{-1} due to -N=N- vibration are showed blue shift in all the metal complexes compared to free ligand, implying the coordination through azo nitrogen [17]. Furthermore, the appearance of new band in the region of 591-554 cm^{-1} corresponds to the metal-oxygen bond and frequency at 683-602 cm^{-1} due to metal-nitrogen bond, which supports the contribution of nitrogen and oxygen in the coordination. In complex the appearance of strong band at 3431-3422 cm^{-1} attributed to water molecule this was strongly supported the appearance of new band at 999 cm^{-1}. These overall IR data proposed that the -N=N- and carboxylate O groups were involved in coordination in the metal complexes with bidentate mode.

UV-Visible studies: The assignments of the observed absorption bands of the azo dye and its metal complexes are shown in Table-1. The electronic spectra of the studied ligand in DMSO (10^{-3} M) shown two absorption bands at λ_{max} 299 nm (n→π*) and 383 nm (π→π*). The Cu(II) complex shows three electronic absorption bands at 305, 322, 411 nm, which are assigned as $^2B_{1g} \rightarrow {}^2A_{1g}$ (ν_1), $^2B_{1g} \rightarrow {}^2B_{2g}$ (ν_2), $^2B_{1g} \rightarrow {}^2E_g$ (ν_3) (Fig. 1). The observation of this band suggested a square planar geometry around the Cu(II) ion [18]. In the electronic spectra of Co(II) complex shows three bands, which are assigned $^4T_{1g}$ (F) → $4T_{2g}$ (F) (ν_1), $^4T_{1g}$ (F) → $^4A_{2g}$ (F) (ν_2) and $^4T_{1g}$ (F) → $^4T_{2g}$ (P) (ν_3) transitions. The position of these bands conforms the octahedral geometry for Co(II) complex. The electronic spectrum of Ni(II) complex shows broad band at 304 and 414 nm. These bands may be assigned to the INCT and $^1A_{1g} \rightarrow {}^1B_{1g}$ transitions. These transitions suggested the square planar geometry around Ni(II) ion [19].

TABLE-1
UV-VISIBLE SPECTRA OF THE SYNTHESIZED LIGAND AND METAL COMPLEXES

Compound	λ_{max} (nm)	Transition
L	299, 383	n–π*, π–π*
Cu(II) complex (**1a**)	305, 322, 411	$^2B_{1g} \rightarrow {}^2A_{1g}$ (ν1), $^2B_{1g} \rightarrow {}^2B_{2g}$ (ν2), $^2B_{1g} \rightarrow {}^2E_g$ (ν3)
Co(II) complex (**1b**)	292, 306, 387	$^4T_{1g}$ (F) → $^4T_{2g}$ (F) (ν1), $^4T_{1g}$(F) → $^4A_{2g}$ (F) (ν2), $^4T_{1g}$ (F) → $^4T_{2g}$ (P) (ν3)
Ni(II) complex (**1c**)	304, 414	INCT $A^1_{1g} \rightarrow B^1_{1g}$

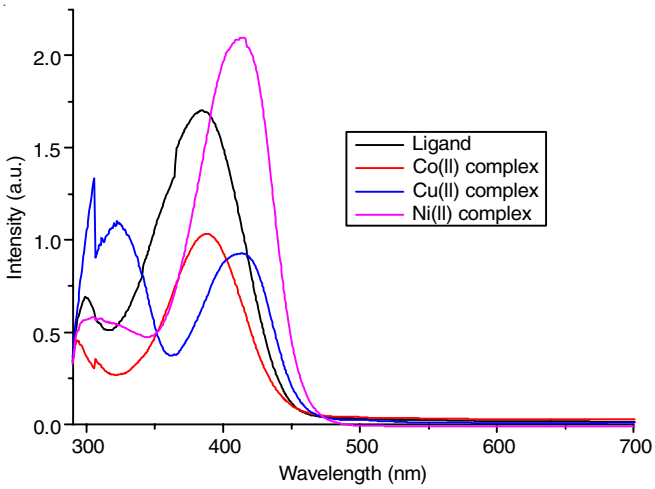

Fig. 1. UV-visible spectra of azo ligand and its metal complexes

Thermal studies: Thermogravimetric analysis of the metal(II) complexes were studied in a temperature range from 30 to 900 ºC at a scan rate of 10 ºC/min in nitrogen atmosphere on TG-DSC curves. All the prepared metal complexes of azo dye exhibited high thermal stability (Fig. 2). The Cu(II) complex shows three stages of disintegration. The first stage resembles to the loss of pyridine ring of the ligand with a weight loss of 18.88% (calcd. 18.97%) at temperature range of 30.0-346.89 ºC. At temperature 347-355 ºC with a loss of 23.44% (calcd. 23.55%) was observed in the second stage, after the elimination of the fragments of azo-ligand the decomposition of the remaining portion of the metal complex started simultaneously between temperature 355.68-367.0 ºC with a weight loss of 32.95% (calcd. 33.14%). A further heating up to 900 ºC and the stable metal oxide CuO was formed (Table-2).

The TGA of Co(II) complex also showed three stages of decomposition. In the first step, the loss of coordinated water molecule was takesplace at temperature 66 ºC. The second step involves the loss of some portion of the ligand ($C_8H_5N_3$) takes place with a loss of 22.7% (calcd. 22.5%) at temperature range of 67 to 351 ºC. In the third stage, the dissociation of

TABLE-2
THERMAL DECOMPOSITION OF METAL COMPLEXES AT NITROGEN

Complexes	Stages	Decomposition temp. (°C)	Probable assignment	Loss of mass in (%)	Residual species
Cu(II) complex (**1a**)	1st	30-346	$C_8H_8N_4$	18.88	CuO
	2nd	347-355	$S_2O_4N_2H_2$	23.44	
	3rd	Above 356	$C_4H_8N_4O_4$	32.95	
Co(II) complex (**1b**)	1st	30-66	$2\ H_2O$	4.1	CoO
	2nd	67-351	$C_8H_8N_3$	22.76	
	3rd	Above 357	$C_4H_8N_4O_8S_2$	47.16	
Ni(II) complex (**1c**)	1st	30-95	$2H_2O$	4.1	NiO
	2nd	96-343	$C_8H_8N_4$	19.2	
	3rd	344-351	$H_4N_2O_4S_2$	23.7	
	4th	352-750	$C_4H_8N_4O_4$	40.3	

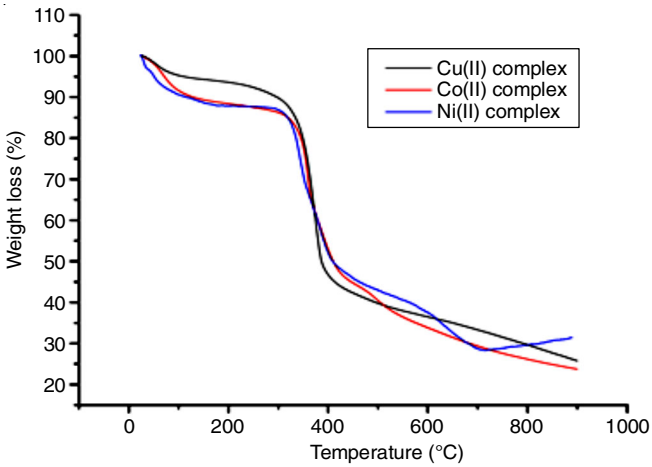

Fig. 2. Thermal decomposition of the synthesized metal complexes (**1a-c**)

complete ligand occured in the temperature range of 352-800 ºC, which corresponds to $C_4H_8N_4O_8S_2$ with a mass loss 47.11% (calcd. 47.16%) leaving behind the stable CoO as a residue. Similarly, the thermogravimetric analysis of Ni(II) complex, the first stage corresponds to the loss of water with a loss of 4.1% (calcd. 4%) at 95 ºC. In second stage, the loss of two pyridine groups was taken place with a mass loss 19.2% (calcd. 19.17%) at the temperature range of 96-343 ºC. The loss of SO_2NH was taken place in the third step with a loss of 23.52% (calcd. 23.70%) in the temperature range of 344-351 ºC. The final step the decomposition was occurred with 40.2% loss (calcd. 40.30%) at a temperature range of 352 to 750 ºC due to the complete decomposition of organic part leaving behind one mole of NiO.

SEM-EDAX studies: To study the surface morphology and to determine the elements present on the surface of the ligand and its metal complexes were analyzed using scanning electron microscope with EDAX analysis. The SEM images with EDX spectra are shown in Fig. 3. For azo-ligand, the broken ice like structured particles were observed. Small granules like structure was observed for Ni(II) complex, while for Co(II) complex layer by layer chip like structure was observed. In case of copper(II) complex, uniformed granules were formed. Therefore, clear changes in the structure of the ligand after the formation of metal complex were detected by using SEM [20]. The EDX analysis of metal complexes showed the metal content along with nitrogen, carbon, and oxygen proposing the formation of metal complex.

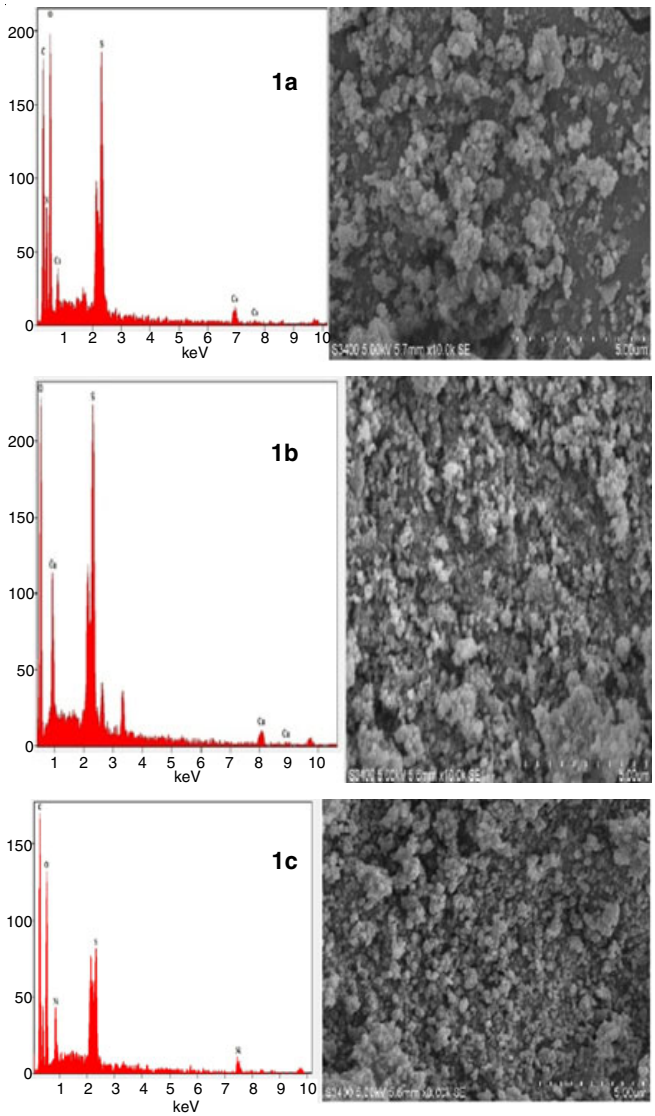

Fig. 3. SEM-EDAX spectrum of the synthesized metal complexes (**1a-c**)

XRD studies: The degree of crystallinity of the azo-metal chelates were studies by powdered XRD. The XRD pattern of metal complexes is depicted in Fig. 4. The XRD pattern of Cu(II) complex is shown in Table-3. The XRD pattern of Cu(II) complexes showed seven reflections in the range 9 to 40º (2θ). By using Bragg's equation [2dsin θ = nλ], the inter planar spacing was calculated. The miller indices (*h k l*) values were evaluated and the unit cell parameters were also determined.

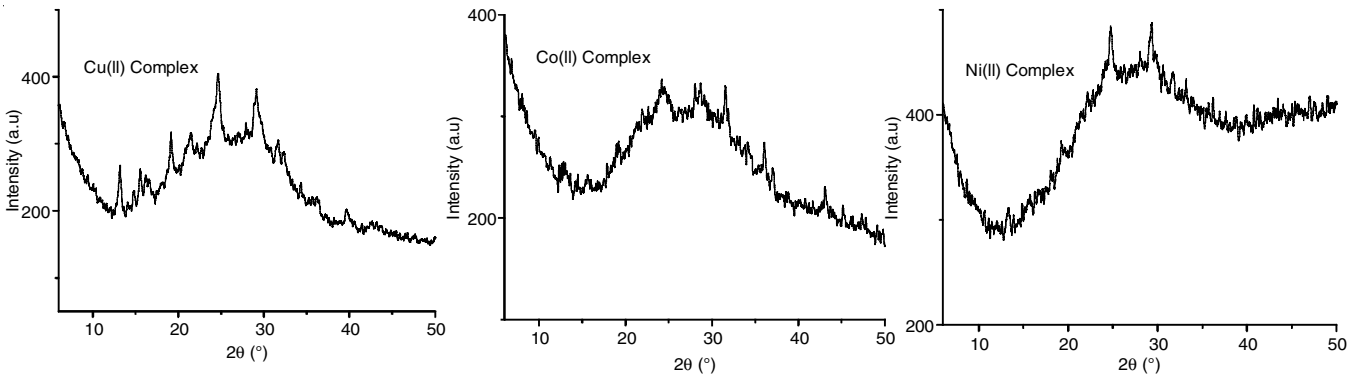

Fig. 4. Powdered XRD patterns of the synthesized metal complexes

TABLE-3
POWDER X-RAY SPECTRAL DATA OF Cu(II) COMPLEX (**1a**)

2θ	θ	sin θ	$\sin^2\theta$	$\sin^2\theta \times 1000$	$h^2 + k^2 + l^2$	*h k l*	D	a (Å)
13.1	6.55	0.114	0.01301	13.01	1	100	6.7570	5.440
19.17	9.58	0.1664	0.02769	27.69	2.1(2)	110	4.629	5.275
22.24	11.12	0.1928	0.03719	37.19	2.8(3)	111	2.0712	5.384
24.75	12.37	0.2142	0.04589	45.89	3.51(4)	200	3.594	5.419
29.07	14.535	0.2509	0.06294	62.94	4.8(5)	210	3.070	5.419
32.42	16.2	0.2789	0.07783	77.83	5.9(6)	211	2.7619	5.401
34.30	17.15	0.2948	0.08695	86.95	6.68(7)	–	2.6129	5.401

The lattice parameters was found to be $a = b = c = 5.44$ Å. The calculated $h^2+k^2+l^2$ was 1,2,3,4,6,7. The forbidden number 7 indicates complex belongs to hexagonal or tetragonal system [21].

Similarly, the above calculations were carried out for the Co(II) and Ni(II) complexes showed 9 and 6 reflections at 7-40º. The XRD patterns of Co(II) and Ni(II) metal chelates are depicted in Tables 4 and 5. The $h^2+k^2+l^2$ values of Co(II) were 1,2,3,4,6,8,10,14,15, while for Ni(II) complex the values were 1,1,4,5,6,7. The existence of forbidden numbers like 15 for Co(II) complex and 7 for Ni(II) complex confirmed that both complexes may belong to the hexagonal or tetragonal systems. The calculated lattice parameters for Co(II) were $a = b = c =$ 7.4 Å, while for Ni(II) complexes were $a = b = c = 5.4$ Å, respectively.

Antimicrobial activity: The potency of the metal chelates with the reference drugs amoxicillin (antibacterial drug) and fluconazole (antifungal drug) were tested against Gram-positive (*S. aureus*), Gram-negative (*E. coli*, *X. ampestris*, *K. pneumonia*) bacteria and two fungal strains (*C. albicans* and *A. flavus*). The zone of inhibition (mm) was used to compare the antimicrobial activity of the synthesized compounds with reference drug.

TABLE-4
POWDER X-RAY SPECTRAL DATA OF Co(II) COMPLEX (**1b**)

2θ	θ	sin θ	$\sin^2\theta$	$\sin^2\theta \times 1000$	$h^2 + k^2 + l^2$	*h k l*	D	a (Å)
9.6	4.8	0.0836	0.0070	7.0	1	100	9.214	7.416
14.4	7.2	0.1253	0.0157	15.7	2.24(2)	110	6.1476	7.410
17.92	8.96	0.1557	0.02406	24.06	3.4(3)	111	4.9473	7.377
19.17	9.58	0.1655	0.0276	27.6	3.9(4)	200	4.6543	7.37
23.03	11.51	0.1995	0.0398	39.8	5.68(6)	211	3.8611	7.412
28.06	14.03	0.2424	0.05877	58.77	8.39(8)	220	3.1778	7.414
31.54	15.52	0.2675	0.07159	71.59	10.22(10)	310	2.8796	7.415
36.04	18.02	0.3093	0.09569	95.69	13.67(14)	321	2.4904	7.397
36.95	18.47	0.3168	0.10036	100.36	14.5(15)	--	2.4315	7.341

TABLE-5
POWDER X-RAY SPECTRAL DATA OF Ni(II) COMPLEX (**1c**)

2θ	θ	sin θ	$\sin^2\theta$	$\sin^2\theta \times 1000$	$h^2 + k^2 + l^2$	*h k l*	D	a (Å)
13.18	6.59	0.1147	0.01317	13.17	1(1)	100	6.7157	5.40
19.31	9.655	0.1676	0.02809	28.09	2.1(1)	110	4.5960	5.42
24.82	12.41	0.2149	0.04618	46.18	3.52(4)	200	3.5844	5.41
29.35	14.675	0.2533	0.06479	64.17	4.8(5)	210	3.0410	5.43
31.58	15.79	0.2721	0.07404	74.04	5.65(6)	211	2.8309	5.42
33.25	16.62	0.2861	0.08185	81.85	6.61(7)	–	2.6924	5.41

TABLE-6
ANTIBACTERIAL ACTIVITY OF METAL COMPLEXES

Bacteria		$[Cu(L)_2]$	$[Co(HL_2)2(H_2O)]$	$[Ni(HL_2)]2(H_2O)$
Staphylococcus aureus	25 mg/mL	06	13	02
	50 mg/mL	12	14	06
	100 mg/mL	18	22	11
	Amoxicillin	14	15	11
E. coli,	25 mg/mL	04	7.5	02
	50 mg/mL	16	12	05
	100 mg/mL	19	17.5	10
	Amoxicillin	17	15	13
Xanthomonas ampestris	25 mg/mL	03	08	01
	50 mg/mL	12	16	06
	100 mg/mL	13	17	09
	Amoxicillin	14	21	08
Klebsiella pneumonia	25 mg/mL	05	12	03
	50 mg/mL	11	14	12
	100 mg/mL	15	19	14
	Amoxicillin	17	15	12

Results of the antimicrobial activity are presented in Table-6. It is observed that all the metal chelates exhibited significantly enhanced the antibacterial activity against selected bacterial strains. In general, the *in-vitro* bacterial activity of Co(II) and Cu(II) exhibited higher antibacterial activity than Ni(II) complex.

Moreover, towards fungi species the metal chelates are more active than the standard drug, with Ni(II) complex being highly active. Whereas ligand shows the least activity compared to all synthesized metal complexes against both strains (Table-7). An increase in the pharmacological activity could be due to the electron delocalization within the metal complexes occurs this will reduces the polarity of the metal ions. Polarity decrease due to the sharing of positive charge with the ligand donor atoms. This may upsurge the hydrophobic and lipophilic character of the metal complex, permitting it to the lipid layer of the organism killing them more effectively [22].

TABLE-7
ANTIFUNGAL ACTIVITY RESULTS OF THE LIGAND AND ITS METAL COMPLEXES

Compounds	Inhibition (%)			
	C. albicans		*A. flavus*	
	50 µg/mL	100 µg/mL	50 µg/mL	100 µg/mL
L	22 ± 0.20	41 ± 0.27	19 ± 0.46	46 ± 0.31
$[Cu(L)_2]$	38 ± 0.25	62 ± 0.15	25 ± 0.21	67 ± 0.22
$[Co(HL_2)(H_2O)_2]$	32 ± 0.33	64 ± 0.21	31 ± 0.64	66 ± 0.32
$[Ni(HL_2)]2(H_2O)$	37 ± 0.14	68 ± 0.33	41 ± 0.13	78 ± 0.21
Fluconazole	39 ± 0.13	79 ± 0.13	37 ± 0.14	89 ± 0.13

Values are symbolized as the mean ± SEM.
Values are significant for the standard at 0.005 level of significance.

Molecular docking: All the synthesized metal complexes were employed to recognize the interaction between the metal complexes and the target receptor. The docking studies showed significance interaction with the target receptor RpsA. All the metal chelates showed well recognized aquaphobic interactions such as His322, Ile349, Glu325, Ser359, Arg355, Asp350, Arg357 Asp352, Arg357 and Gln3649 in the target enzyme active pockets (Fig. 5). The relative binding affinities of all the

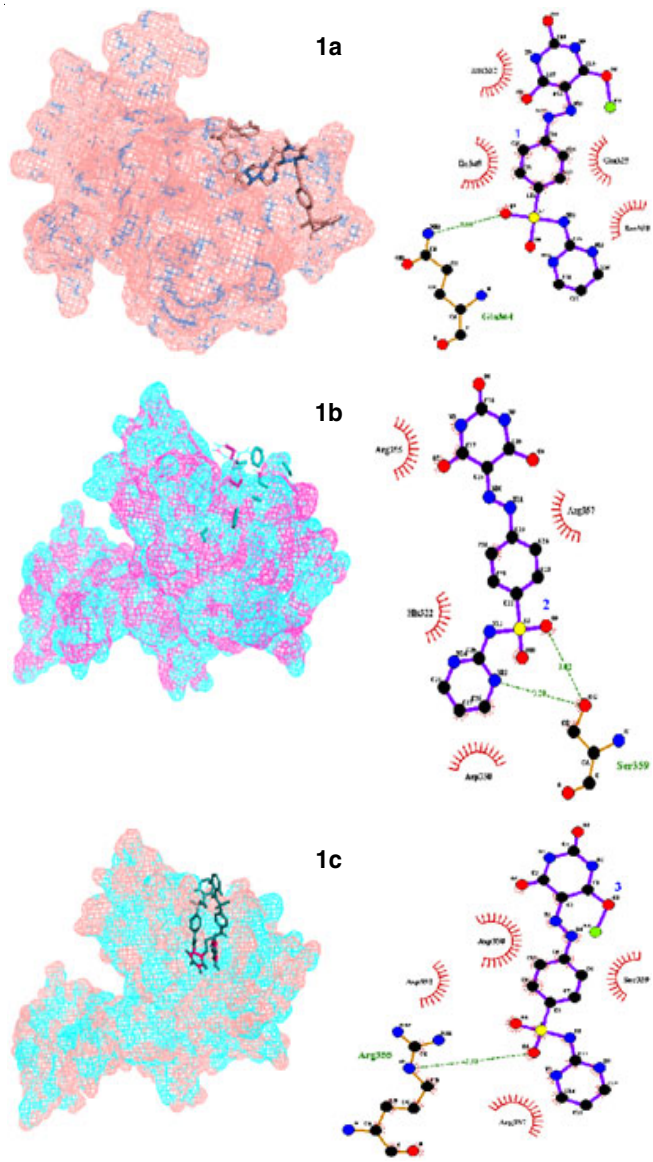

Fig. 5. Three-dimensional representation of the metal complex (**1a-c**) into active protein RpsA

TABLE-8
DOCKING ENERGY DATA OF THE SYNTHESIZED COMPLEXES (**1a-c**)

Compounds	Binding energy (kcal/mol)	H-bonds	H-bond length (Å)	H-bond with	Hydrophobic interactions
1a	-2.51	1	3.08	Gln364	His 322, Ile349, Glu325, Ser359
1b	-3.90	2	3.02, 3.20	Ser359, Ser359	Arg355, His322, Asp350, Arg357
1c	-3.45	1	2.51	Arg355.	Asp352, Asp350, Ser359, Arg357

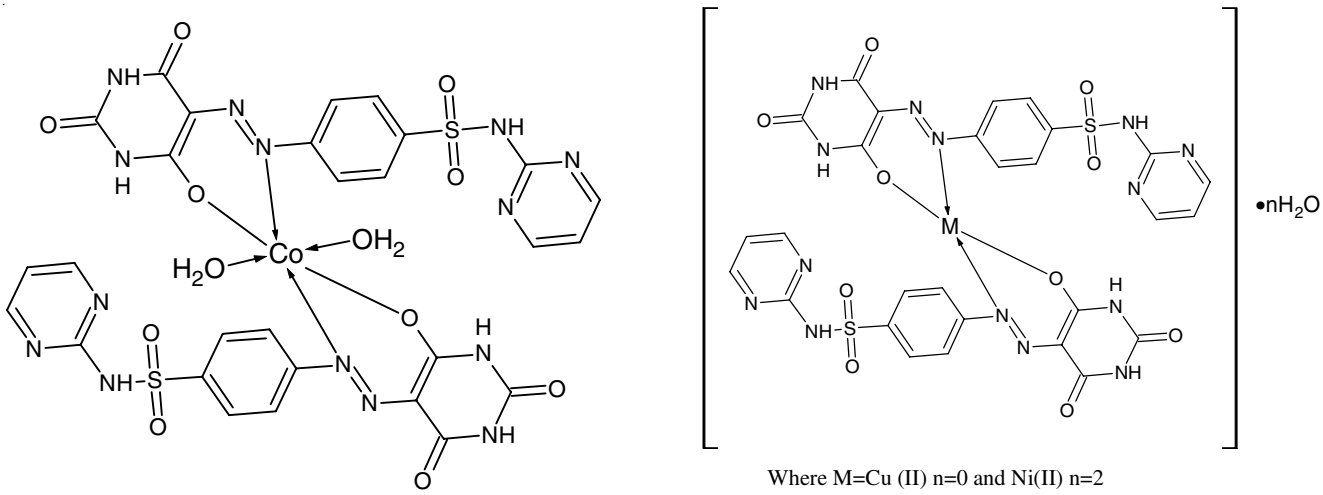

Where M=Cu (II) n=0 and Ni(II) n=2

Fig. 6. Structure of metal complexes

metal complexes were accomplished in the range of -2.51 kcal/mol to -3.90 kcal/mol, respectively (Table-8). From the results, Co(II) complex shows the highest negative relative binding energy, which indicated that it may be considered as a good inhibitor glucoseamine-6-phosphate synthase.

Conclusion

A successful synthesis of novel azo derivative of sulfadiazine with their Cu(II), Co(II) and Ni(II) complexes was achieved with good yield. All the synthesized metal compounds were characterized by spectroscopic and analytical techniques. From elemental analysis and mass spectroscopic measurements, it was determined that the metal to ligand ratio is 1:2 stoichiometry of the type [ML_2]. Based on the results, Cu(II) and Ni(II) complexes exhibits square planar geometry, whereas Co(II) ion in the complex adopts a octahedral environment. The tentative structures of the synthesized complexes are shown in Fig. 6. Thermal results showed the high thermal stability and suggested molecular formulae of the complexes. Metal complexes were tested against Gram-negative bacteria, Gram-positive bacteria and two strains of fungi, all the complexes showed enhanced activity against standard drug and can be used as a potent antimicrobial agent against selective pathogens. Molecular docking studies were carried out to explore the binding interactions between the synthesized complex and the target receptor RpsA. It showed that the tested compounds fit into the receptor active site with complimentary binding energy.

CONFLICT OF INTEREST

The authors declare that there is no conflict of interests regarding the publication of this article.

REFERENCES

1. M. Hassan, S.M. Nasr, S.E. Abd-El Razek, M.S. Abdel-Aziz and S.M. El-Gamasy, *Arab. J. Chem.*, **13**, 7324 (2020); https://doi.org/10.1016/j.arabjc.2020.08.010
2. M. Rocha, O.E. Piro, G.A. Echeverría, A.C. Pastoriza, M.A. Sgariglia, J.R. Soberón and D.M. Gil, *J. Mol. Struct.*, (2018); https://doi.org/10.1016/j.molstruc.2018.09.008
3. T.N.J.I. Edison, R. Atchudan, M.G. Sethuraman and Y.R. Lee, *J. Photochem. Photobiol. B*, **162**, 604 (2016); https://doi.org/10.1016/j.jphotobiol.2016.07.040
4. K.J. Al-Adilee and H.A.K. Kyhoiesh, *J. Mol. Struct.*, **1137**, 160 (2017); https://doi.org/10.1016/j.molstruc.2017.01.054
5. Y.K. Abdel-Monem, S.A. Abou El-Enein and M.M. El-Sheikh-Amer, *J. Mol. Struct.*, **1127**, 386 (2017); https://doi.org/10.1016/j.molstruc.2016.07.110
6. H.E. Gaffer, *Color. Technol.*, **135**, 484 (2019); https://doi.org/10.1111/cote.12437
7. B.R. Kirthan, M.C. Prabhakara, H.S. Bhojyanaik, P.H. Amith Nayak, R. Viswanath, H.B. Teja and Ereshanaik, *Inorg. Chem. Commun.*, **135**, 109109 (2022); https://doi.org/10.1016/j.inoche.2021.109109
8. P.A. Ajibade, G.A. Kolawole, P. O'Brien, M. Helliwell and J. Raftery, *Inorg. Chim. Acta*, **359**, 3111 (2006); https://doi.org/10.1016/j.ica.2006.03.030
9. A. Mohammadi and M. Safarnejad, *Spectrochim. Acta A Mol. Biomol. Spectrosc.*, **126**, 105 (2014); https://doi.org/10.1016/j.saa.2014.02.010
10. P.H. Amith Nayak, H.S. Bhojya Naik, H.B. Teja, B.R. Kirthan and R. Viswanath, *J. Electron. Mater.*, **50**, 2090 (2021); https://doi.org/10.1007/s11664-020-08728-0
11. A. Shaikh and J.S. Meshram, *Cogent Chem.*, **1**, 1019809 (2015); https://doi.org/10.1080/23312009.2015.1019809
12. K. El-Baradie, R. El-Sharkawy, H. El-Ghamry and K. Sakai, *Spectrochim. Acta A Mol. Biomol. Spectrosc.*, **121**, 180 (2014); https://doi.org/10.1016/j.saa.2013.09.070
13. P.H. Amith Nayak, H.S. Bhojya Naik, H.B. Teja, B.R. Kirthan and R. Viswanath, *Mol. Cryst. Liq. Cryst.*, **722**, 67 (2021); https://doi.org/10.1080/15421406.2020.1868053

14. N. Venugopal, G. Krishnamurthy, H.S. Bhojyanaik and P. Murali Krishna, *J. Mol. Struct.*, **1183**, 37 (2019); https://doi.org/10.1016/j.molstruc.2019.01.031
15. R. Gup, E. Giziroglu and B. Kirkan, *Dyes Pigments*, **73**, 40 (2007); https://doi.org/10.1016/j.dyepig.2005.10.005
16. H.B. Teja, H.S. Bhojya Naik, P.H. Amith Nayak and M.C. Prabhakara, *Asian J. Chem.*, **33**, 1709 (2021); https://doi.org/10.14233/ajchem.2021.23178
17. N. Venugopal, G. Krishnamurthy, H.S. Bhojya Naik and J.D. Manohara, *J. Inorg. Organomet. Polym. Mater.*, **30**, 2608 (2020); https://doi.org/10.1007/s10904-019-01394-8
18. N.M. Mallikarjuna, J. Keshavayya and B.N. Ravi, *J. Mol. Struct.*, **1173**, 557 (2018); https://doi.org/10.1016/j.molstruc.2018.07.007
19. N.M. Mallikarjuna, J. Keshavayya, M.R. Maliyappa, R.A. Shoukat Ali and T. Venkatesh, *J. Mol. Struct.*, **1165**, 28 (2018); https://doi.org/10.1016/j.molstruc.2018.03.094
20. S.M. El-Megharbel, A.S. Megahed and M.S. Refat, *J. Mol. Liq.*, **216**, 608 (2016); https://doi.org/10.1016/j.molliq.2016.01.097
21. B.G. Devika, B.H. Doreswamy, N.M. Mallikarjuna and H.C. Tandon, *J. Mol. Struct.*, **1185**, 69 (2019); https://doi.org/10.1016/j.molstruc.2019.02.029
22. D.S.Y. Gaëlle, D.M. Yufanyi, R. Jagan and M.O. Agwara, *Cogent Chem.*, **2**, 1253201 (2016); https://doi.org/10.1080/23312009.2016.1253201